

Variability in the summer season hydrological cycle over the Atlantic-Europe region 1979–2007

Richard P. Allan^{a*} and Igor I. Zveryaev^b

^a *Environmental Systems Science Centre, University of Reading, Reading, Berkshire, UK*

^b *Sea Atmosphere Interaction And Climate Laboratory, PP Shirshov Institute of Oceanology, Moscow, Russia*

ABSTRACT: Variability in aspects of the hydrological cycle over the Europe-Atlantic region during the summer season is analysed for the period 1979–2007, using observational estimates, reanalyses and climate model simulations. Warming and moistening trends are evident in observations and models although decadal changes in water vapour are not well represented by reanalyses, including the new European Centre for Medium Range Weather Forecasts (ECMWF) Interim reanalysis. Over the north Atlantic and northern Europe, observed water vapour trends are close to that expected from the temperature trends and Clausius–Clapeyron equation ($7\% K^{-1}$), larger than the model simulations. Precipitation over Europe is dominated by large-scale dynamics with positive phases of the North Atlantic Oscillation coinciding with drier conditions over north Europe and wetter conditions over the Mediterranean region. Evaporation trends over Europe are positive in reanalyses and models, especially for the Mediterranean region (1–3% per decade in reanalyses and climate models). Over the north Atlantic, declining precipitation combined with increased moisture contributed to an apparent rise in water vapour residence time. Maximum precipitation minus evaporation over the north Atlantic occurred during summer 1991, declining thereafter. Copyright © 2010 Royal Meteorological Society

KEY WORDS *hydrological cycle; Europe; water; precipitation; satellite; climate models*

Received 4 May 2009; Revised 18 November 2009; Accepted 19 November 2009

1. Introduction

The global water cycle determines the availability of fresh water and impacts society and ecosystems through severe weather, flooding and droughts. Large and relatively fast changes in the hydrological cycle may result in catastrophic consequences. This is especially true for densely populated regions, such as Europe where temperature is likely to increase faster than the global mean. The hydrological response is more complex, with projected increases in precipitation over northern Europe yet decreases for the Mediterranean, with substantial seasonal dependence (Christensen *et al.* 2007). Recent analysis suggests that global and regional changes in the hydrological cycle are already underway (e.g. Wentz *et al.* 2007; Allan and Soden 2007; Yu and Weller 2007; Lenderink and Van Meijgaard 2008). It is therefore important to monitor and understand variability in aspects of the hydrological cycle over the Europe-Atlantic region using observationally derived estimates.

Traditionally, studies of climate variability in the Atlantic-European sector have focused on the winter season, characterized by the large anomalies in atmospheric circulation associated with the North Atlantic Oscillation (NAO) (Trenberth *et al.* 2007). There is significant

seasonality in variability of precipitation (P) and column integrated water vapour (CWV) in the European region (Zveryaev 2006; Zveryaev *et al.* 2008). Moreover, recent climate extremes, such as the 2003 European summer heatwave (Schar *et al.* 2004) and 2007 UK flooding (Blackburn *et al.* 2008), as well as projected increases in their occurrence (Christensen *et al.* 2007, Pal *et al.* 2004), point to the importance of understanding mechanisms driving variability of European climate during the warm season (Folland *et al.* 2009). There is evidence of complexity in variability of summertime atmospheric moisture over Europe and in its relationships with other key climate parameters (Zveryaev *et al.* 2008). Therefore, it is crucially important to (1) monitor changes in aspects of hydrological cycle, (2) quantify variability and (3) understand processes through which the hydrological cycle impacts European climate during summer.

Previous work has demonstrated increasing surface moisture trends over large areas of the globe (Trenberth *et al.* 2005; Dai 2006; Willett *et al.* 2008), including the Atlantic-Europe sector. Over Europe, the moistening is thought to have provided a strong positive feedback to warming which is likely to have been forced both by increased greenhouse gases and reduced aerosol (Philipona *et al.* 2009) but is also related to longer term changes in the Atlantic Multi-decadal Oscillation (e.g. Sutton and Hodson 2005). Relationships between temperature, moisture and precipitation (e.g. Dai 2006; Trenberth and Shea 2005) and experiments with regional

* Correspondence to: Richard P. Allan, Environmental Systems Science Centre, Harry Pitt Building, Whiteknights, University of Reading, Reading, Berkshire, UK. E-mail: r.p.allan@reading.ac.uk

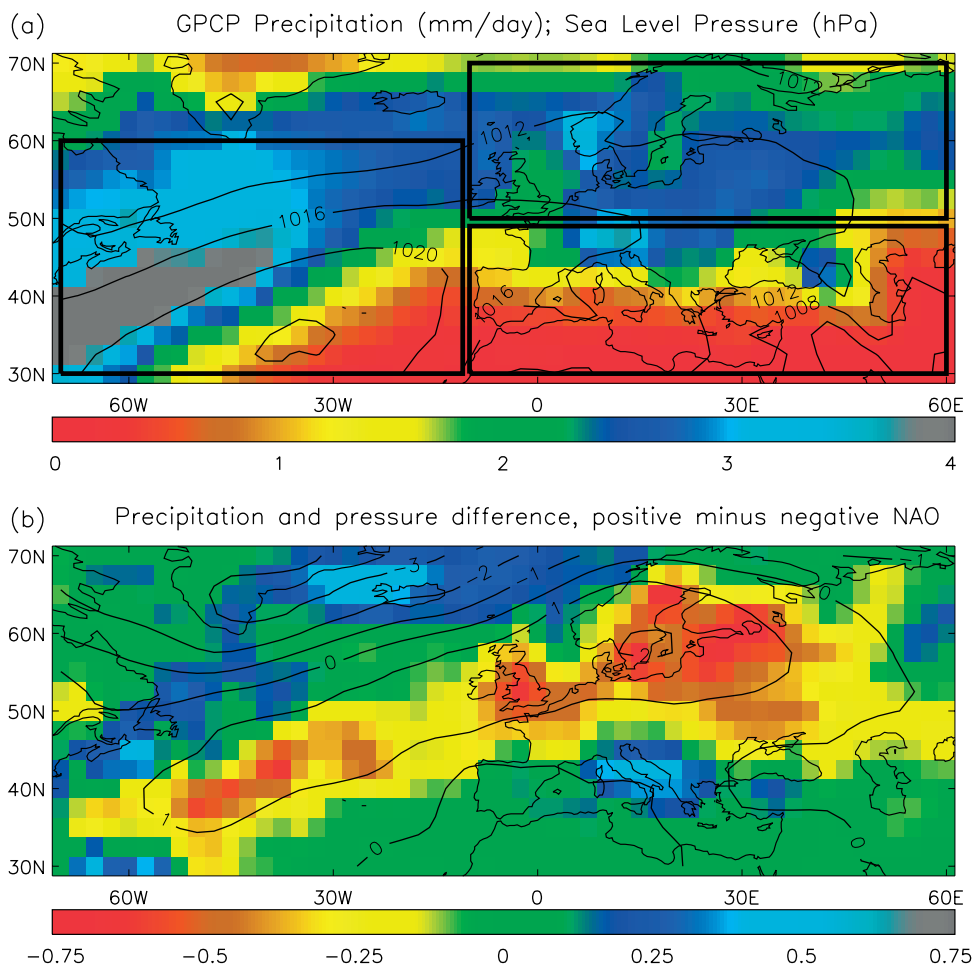


Figure 1. June–August (a) climatology of precipitation (colours) and mean sea level pressure (contours) and (b) differences in precipitation (colours) and mean sea level pressure (contours) for positive minus negative phases of the North Atlantic Oscillation. Boxes denote the regions of detailed study (north Atlantic, north Europe and Mediterranean).

models (Schär *et al.* 1999; Koster *et al.* 2004) have been used to understand processes important in determining responses of the regional water cycle to warming and moistening.

The present paper seeks to monitor and quantify recent variability in aspects of the hydrological cycle specifically for the Europe–Atlantic region summer season, utilizing a variety of datasets and products including surface temperature, surface and column water vapour, precipitation and evaporation. We inter-compare observational estimates with climate model simulations and reanalysis products over the period 1979–2007. The aim is to quantify variability, detect significant trends over the period and assess robustness of relationships between aspects of the hydrological cycle.

2. Datasets

We consider the Europe–Atlantic region depicted in Figure 1 which displays June–August mean precipitation from the Global Precipitation Climatology Project (GPCP; Adler *et al.* 2008) and sea level pressure (contours) from the National Center for Environmental Prediction reanalysis (NCEP; Kalnay *et al.* 1996) over

the period 1979–2007. This region sub-divided into a north Atlantic area (10°–70°W, 30°–60°N) centred on the high precipitation storm-track region, a north Europe region of consistently moderate precipitation (10°W–60°E, 50°–70°N) and a Mediterranean region characterized by a strong gradient in P from moderate values in the north to the dry south (10°W–60°E, 30°–50°N). For all datasets, June–August means are considered.

2.1. Observationally derived products

For precipitation we consider GPCP data over land and ocean (Figure 1) which is available on a $2.5^\circ \times 2.5^\circ$ grid. These data combine infrared radiances from geostationary and polar orbiting satellites with rain gauge data since 1979, with the inclusion of microwave-based estimates from the Special Sensor Microwave Imager (SSM/I) since 1988 (Adler *et al.* 2008). Ocean-only satellite retrievals from SSM/I (Wentz *et al.* 2007) are also considered separately for the period 1988–2007, using the F08–F11–F13 satellite series, considering $1^\circ \times 1^\circ$ data, averaged from the $0.25^\circ \times 0.25^\circ$ dataset using a missing data tolerance of 30%.

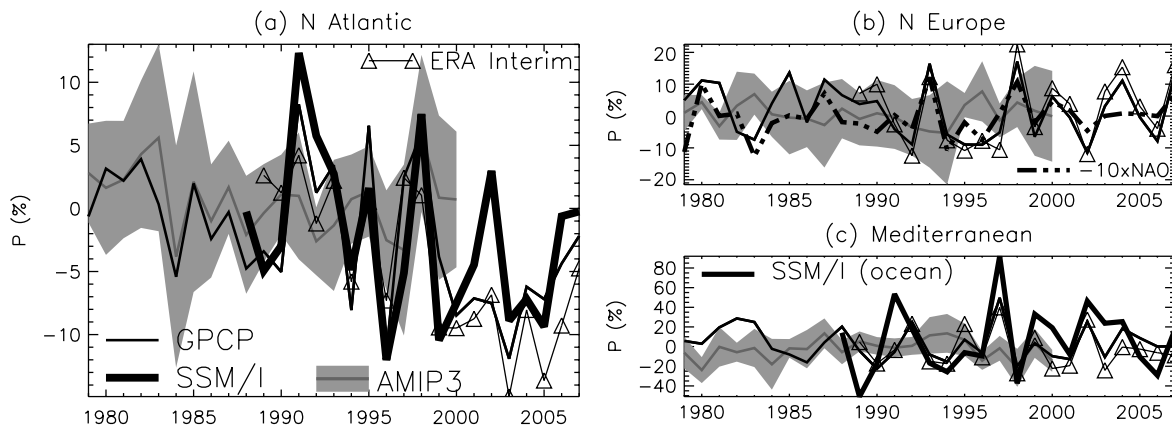


Figure 2. Time series of summer season precipitation anomalies (%) for the (a) north Atlantic, (b) north Europe and (c) Mediterranean regions as defined in Figure 1. Also shown in (b) is the North Atlantic Oscillation index multiplied by -10 .

Observed surface temperature (T_s) is taken from the Hadley Centre global sea Ice and Sea Surface Temperature (HadISST) data set over the ocean (Rayner *et al.* 2003) and from the Hadley Centre/Climatic Research Unit T_s anomaly dataset (HadCRUT3; Brohan *et al.* (2006)) over land. The land data is derived from homogenized, quality-controlled, monthly averaged temperatures, with additional removal of duplicate records and bad values based upon comparison with reanalysis data, augmented by visual inspection. Data are provided on a $5^\circ \times 5^\circ$ grid, compiled from all station anomalies within the domain but excluding station outliers in excess of five standard deviations.

CWV and wind speed over the oceans are from SSM/I as described by Wentz *et al.* (2007); in addition observed near-surface specific humidity is taken from the Hadley Centre/Climatic Research Unit humidity dataset (HadCRUH; Willett *et al.* 2008) over land and ocean (1979–2003). These data were based upon quality-controlled dry-bulb and dewpoint depression temperature measurements which were converted to specific humidity. Further details of the homogenization techniques and an analysis of trends are discussed by Willett *et al.* (2008).

Observationally derived evaporation (E) over the Atlantic and Mediterranean is supplied by the Woods Hole Oceanographic Institute (WHOI) on a $1^\circ \times 1^\circ$ grid (Yu and Weller 2007). These data are computed by applying standard bulk aerodynamical formulas, using as input objective analysis of T_s and near-surface temperature, wind speed and specific humidity from satellite retrievals (including SSM/I) and reanalyses, employing *in situ* ship and buoy measurements to prescribe error estimates required to specify weightings to the data within the objective analysis procedure (Yu and Weller 2007).

2.2. Reanalysis products and model simulations

Additional dynamical fields are considered: 500 hPa vertical motion (ω), surface pressure (p_s) and pressure at mean sea level (PMSL), in addition to the variables outlined above, from reanalysis datasets. These are taken from the NCEP reanalysis (1979–2007) and the European Centre for Medium Range Weather Forecasts

40-year reanalysis (ERA40) for 1979–2001 and interim reanalysis (ERA Interim) for 1989–2007 (Uppala *et al.* 2005).

Finally, simulations from atmosphere-only climate models forced with observed sea surface temperature (AMIP3) were taken from the PCMDI archive (www.pcmdi.llnl.gov). Models considered are, the CNRM CM3 (Salas-Méllia *et al.* 2005), the IPSL CM4 (Marti *et al.* 2005), the MIROC high and medium resolution models (version 3.2; Hasumi and Emori (2004)), the MRI CGCM2 version 3.2a (Yukimoto and Noda 2002) and the NCAR CCSM 3.0 (Collins *et al.* 2006), using ensemble member 1 in each case. These models were chosen based on the complete availability of all fields considered in the analysis.

3. Precipitation and dynamical variables

Figure 2 displays percentage anomalies in summer season P over (a) the Atlantic Ocean region, (b) the north European region and (c) the Mediterranean region, defined in Figure 1. The partitioning of northern and southern Europe is deemed appropriate based on previous analysis of the spatial signal in precipitation variability (Zveryaev and Allan 2009; Folland *et al.* 2009) as highlighted by the differences in P between positive and negative phases of the NAO (Figure 1(b)). Anomalies are calculated with respect to the monthly climatology for 1989–1998, chosen due to the availability of all datasets during this period.

Negative trends in P are apparent over the north Atlantic region although this is only statistically significant at the 95% level for GPCP and ERA Interim (Table I). The wettest summer for each dataset was 1991, although this is not captured by the AMIP3 ensemble mean. Although there is positive correlation between GPCP and the AMIP3 ensemble P , this is not statistically significant ($r = 0.3$).

Over northern Europe and the Mediterranean, trends are not significant, in contrast to longer term observed changes (Pal *et al.* 2004), but exhibit substantial

Table I. Trends in aspects of the hydrological cycle over the north Atlantic (ocean), north Europe (land and ocean) and Mediterranean (land and ocean unless stated) regions.

Dataset	Years	Atlantic	North Europe	Mediterranean
<i>dT/dt (K/decade), r</i>				
ERA40	1979–2001	0.19 ± 0.10, 0.40	0.37 ± 0.15, 0.48	0.55 ± 0.10, 0.76
NCEP	1979–2007	0.18 ± 0.07, 0.46	0.39 ± 0.10, 0.60	0.34 ± 0.07, 0.66
HadISST/HadCRUT3	1979–2007	0.26 ± 0.06, 0.62	0.47 ± 0.12, 0.59	0.64 ± 0.07, 0.86
ERA Int	1989–2007	0.35 ± 0.14, 0.53	0.55 ± 0.17, 0.61	0.69 ± 0.15, 0.74
AMIP3	1979–2000	0.20 ± 0.10, 0.41	0.28 ± 0.08, 0.60	0.28 ± 0.07, 0.66
<i>dCWV/dt (%/decade), r</i>				
ERA40	1979–2001	2.68 ± 0.54, 0.73	0.60 ± 1.12, 0.12	0.10 ± 1.21, 0.02
NCEP	1979–2007	1.39 ± 0.34, 0.62	0.78 ± 0.82, 0.18	−1.74 ± 0.72, −0.42
SSM/I	1988–2007	1.71 ± 0.81, 0.45	–	1.91 ± 1.59 ^a , 0.27
HadCRUH	1979–2003	1.78 ± 0.49, 0.60	3.20 ± 0.70, 0.69	2.59 ± 0.51, 0.72
ERA Int	1989–2007	0.36 ± 0.84, 0.10	3.24 ± 1.28, 0.52	−0.48 ± 1.40, −0.08
AMIP3	1979–2000	1.01 ± 0.49, 0.41	1.14 ± 0.45, 0.50	1.73 ± 0.63, 0.52
<i>dE/dt (%/decade), r</i>				
ERA40	1979–2001	−2.45 ± 1.32, −0.38	2.83 ± 0.81, 0.60	1.27 ± 0.63, 0.40
NCEP	1979–2007	−0.47 ± 0.90, −0.10	1.11 ± 1.07, 0.20	2.04 ± 0.71, 0.48
WHOI	1979–2006	−0.09 ± 0.95, −0.02	–	7.28 ± 1.28^a, 0.74
ERA Int	1989–2007	5.88 ± 1.32, 0.73	1.84 ± 1.18, 0.36	2.26 ± 0.82, 0.55
AMIP3	1979–2000	1.41 ± 1.21, 0.25	1.09 ± 0.63, 0.36	3.05 ± 1.05, 0.55
<i>dP/dt (%/decade), r</i>				
GPCP	1979–2007	−2.84 ± 1.09, −0.45	−1.53 ± 1.94, −0.15	−2.03 ± 3.83, −0.10
SSM/I	1988–2007	−3.46 ± 2.43, −0.32	–	7.86 ± 13.6 ^a , 0.14
ERA Int	1989–2007	−7.90 ± 1.68, −0.75	3.84 ± 4.53, 0.20	−3.81 ± 8.25, −0.11
AMIP3	1979–2000	−1.04 ± 0.89, −0.25	−0.31 ± 1.20, −0.06	1.85 ± 3.57, 0.12

±1 Standard error and the correlation coefficient (*r*) of the linear fits are shown, with statistical significance at above the 95% level highlighted in bold. ^a, ocean regions only.

variability, the range in *P* of order 30% over north Europe and 60% over the Mediterranean in observations, reanalyses and model simulations. There is a link between north Europe *P* and the NAO index (Figure 2(b)), with a correlation coefficient, $r = -0.65$. This is in agreement with Folland *et al.* (2009) who find the positive phase of the summer NAO to be linked with warm, dry, and relatively cloud-free conditions over northern Europe and cooler, wetter and cloudier conditions over southern Europe and the Mediterranean. The ERA Interim reanalysis is able to capture the interannual variability in *P* over Europe although this is not true for the climate model ensemble, suggesting that the sea surface temperature forcing is not sufficient for simulating variability in *P* over Europe.

We now present variability in dynamical variables from the reanalyses over the same regions. Vertical motion over the land regions is consistent between datasets (Figure 3(b) and (c)). Comparing with Figure 2(b) and (c), negative ω (stronger ascent) is associated with greater *P*. For GPCP and NCEP, the correlation is statistically significant at the 99.9% level (Table II) highlighting the dependence of large-scale *P* on mean vertical motion over land. For ERA Interim, the relationship is stronger still and also applies over the Atlantic Ocean region; since the ω and *P* fields are generated by the ECMWF model and such a link is unsurprising.

Also apparent from Figure 3(b) and (c) is anti-correlation between Europe and Mediterranean ω . The negative relationship (Figure 4(a)) is statistically significant at the 95% level with stronger ascent over northern Europe associated with weaker ascent (or stronger descent) over the Mediterranean. There is also anti-correlation for *P* anomalies between the same regions (Figure 4(b)) although this is not statistically significant. Stronger but positive correlations are attained when the Mediterranean time series are correlated with the European time series lagged by 1 year (Figure 4(c) and (d)). For example, negative ω and positive *P* anomalies in the Mediterranean appear to be associated with negative ω and positive *P* anomalies over north Europe in the following year. Again, the relationship for *P* is weak and it is not clear whether this occurs by chance or whether a physical mechanism, for example relating to remote sea surface temperature patterns, can explain this correlation. It is most likely that this correlation results from a period of biennial oscillations in vertical motion anomalies over north Europe and the Mediterranean (Figure 3(b) and (c)), also apparent in north Atlantic surface pressure (Figure 3(d)), which is associated with a period of fluctuating NAO index (Figure 2(b)).

Over the north Atlantic region, correspondence between ω from NCEP, ERA40 and ERA Interim is inferior (Figure 3(a)) and relationship with *P* weaker

HYDROLOGICAL CYCLE VARIABILITY OVER ATLANTIC-EUROPE REGION

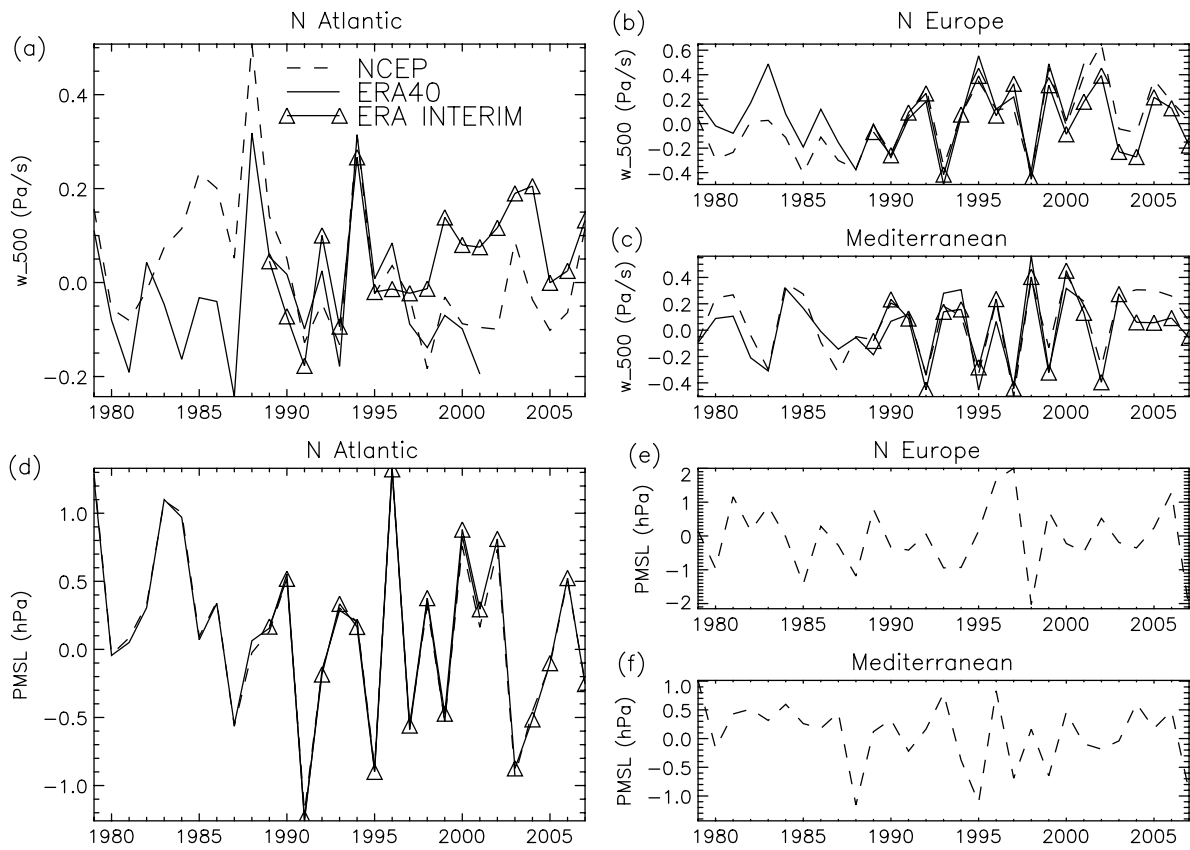


Figure 3. As Figure 2 but for anomalies of 500 hPa vertical motion (Pa/s) and mean sea level pressure (hPa).

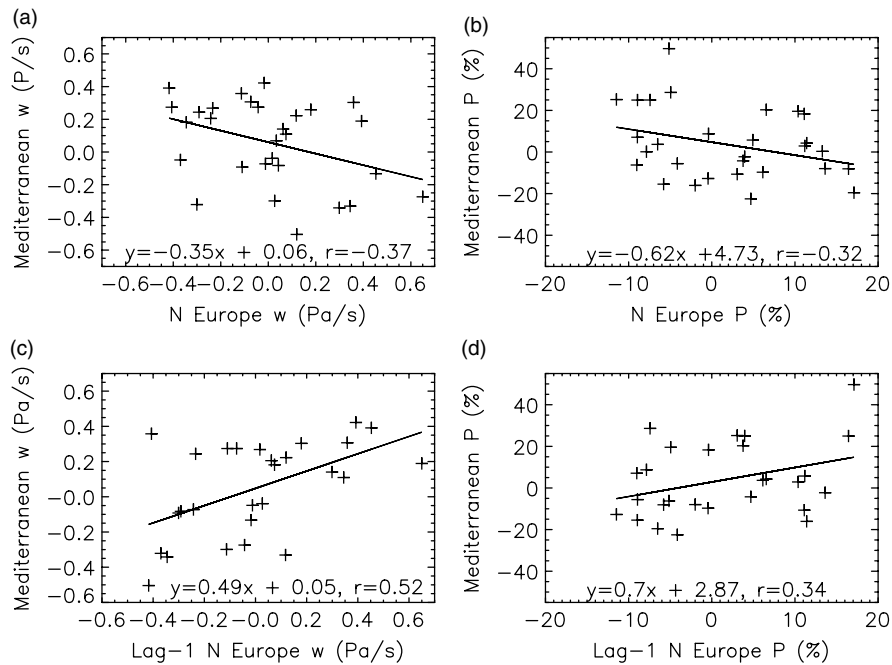


Figure 4. Correlation between north Europe and Mediterranean variables: (a) 500 hPa vertical motion, (b) GPCP precipitation, (c) lag vertical motion (NCEP) and (d) lag precipitation. Lag correlations are calculated by shifting Mediterranean time series forward by 1 year.

(Table II) than the comparisons over land, likely relating to fewer radiosondes over the ocean. Pressure at mean sea level (PMSL) is well constrained among the

reanalyses (Figure f4(d)–(f)); there is correspondence between PMSL and ω over land but not over the north Atlantic region. Correlation between GPCP P and

Table II. Relationships between aspects of the hydrological cycle, surface temperature and vertical motion over the north Atlantic (ocean), north Europe (land and ocean) and Mediterranean (land and ocean unless stated) regions.

Dataset	Years	Atlantic	North Europe	Mediterranean
<i>dCWV/dT</i> (%/K), <i>r</i>				
ERA40	1979–2001	4.74 ± 1.27, 0.63	4.97 ± 0.95, 0.75	1.76 ± 1.64, 0.23
NCEP	1979–2007	4.43 ± 0.69, 0.78	4.49 ± 0.93, 0.68	−0.92 ± 1.52, −0.12
SSM/I, HadISST	1988–2007	5.36 ± 0.79, 0.85	–	2.02 ± 1.70 ^a , 0.27
HadCRUH, HadCRUT3	1979–2003	5.98 ± 0.57, 0.91	3.95 ± 0.65, 0.78	3.55 ± 0.48, 0.84
ERA Int	1989–2007	3.24 ± 1.02, 0.61	5.25 ± 1.07, 0.76	0.75 ± 1.50, 0.12
AMIP3	1979–2000	3.74 ± 0.72, 0.76	2.98 ± 0.89, 0.60	3.99 ± 1.48, 0.52
<i>dE/dT</i> (%/K), <i>r</i>				
ERA40	1979–2001	1.43 ± 2.91, 0.11	3.15 ± 1.11, 0.53	1.21 ± 0.92, 0.28
NCEP	1979–2007	−1.78 ± 2.30, −0.15	1.82 ± 1.63, 0.21	2.61 ± 1.49, 0.32
WHOI, HadISST	1979–2006	2.45 ± 2.14, 0.22	–	7.94 ± 1.98^a, 0.62
ERA Int	1989–2007	6.91 ± 2.44, 0.57	2.68 ± 1.24, 0.47	0.85 ± 1.04, 0.19
AMIP3	1979–2000	7.79 ± 1.85, 0.69	4.66 ± 1.02, 0.72	4.18 ± 2.76, 0.32
<i>dP/dT</i> (%/K), <i>r</i>				
GPCP/NCEP	1979–2007	−3.10 ± 3.06, −0.19	−4.22 ± 2.87, −0.27	−15.9 ± 6.79, −0.41
SSM/I, HadISST	1988–2007	−6.31 ± 3.96, −0.35	–	−4.65 ± 14.5 ^a , −0.08
ERA Int	1989–2007	−7.57 ± 3.41, −0.47	−0.75 ± 5.13, −0.04	−14.0 ± 8.29, −0.38
AMIP3	1979–2000	2.06 ± 1.81, 0.25	−0.53 ± 2.59, −0.05	−5.17 ± 8.13, −0.14
<i>dP/dw</i> (% Pa ^{−1} s), <i>r</i>				
GPCP/NCEP	1979–2007	−9.5 ± 6.6, −0.27	−25.0 ± 3.8, −0.79	−39.7 ± 10.1, −0.60
ERA Int	1989–2007	−32.0 ± 10.3, −0.60	−35.5 ± 4.5, −0.89	−65.2 ± 5.77, −0.94

±1 Standard error and the correlation coefficient (*r*) of the linear fits are shown, with statistical significance at above the 95% level highlighted in bold. ^a, ocean regions only

NCEP PMSL is only significant over the north European sector ($r = -0.65$) and weaker than correlations between P and ω (Table II). Nevertheless, despite low correlation, there is a good agreement between large anomalies of P and PMSL over the north-Atlantic region. In particular, in 1991, enhanced precipitation (Figure 2(a)) was associated with large negative anomalies of PMSL (Figure 3(d)) while negative rainfall anomalies in 1996 were associated with positive PMSL anomalies.

4. Surface temperature, moisture and evaporation

In the previous section, strong dynamical controls on P were identified over land during European summer. We now quantify variability and relationships between different aspects of the hydrological cycle, considering T_s , CWV and E . Figure 5(a)–(c) shows T_s anomalies over the north Atlantic, north Europe and Mediterranean regions. All datasets and regions show pronounced warming trends, ranging from 0.18 K/decade for NCEP over the north Atlantic (1979–2007) to 0.69 K/decade for ERA Interim over the Mediterranean from 1989 to 2007 (Table I). Over the ocean, T_s changes are well constrained by observations for all datasets; lower T_s in HadISST observations during 1979–1980 explain a stronger trend than ERA40 and NCEP. The period 1989–2007 is characterized by a stronger warming trend for all regions, as captured by the ERA Interim dataset. It has been suggested that some of this signal relates to a reduction

in direct and indirect aerosol surface cooling (e.g. Wild *et al.* 2008; Evan *et al.* 2009); this is beyond the scope of the present study. The models simulate the weakest warming trends over Europe, 0.28 K/decade over the period 1979–2000.

Strongly coupled to the warming over the North Atlantic Ocean is an increase in moisture (Figure 5(d)) as demonstrated previously over tropical oceans (e.g. Wentz *et al.* 2007). Observed CWV from SSM/I increases at the rate 1.7%/decade, similar to observed percentage changes in surface specific humidity from HadCRUH (Table I). Trends are weaker in the models while NCEP is thought to underestimate and ERA40 to overestimate trends in CWV over the ocean (Allan *et al.* 2004). ERA Interim produces the weakest trend in CWV, at odds with the SSM/I and HadCRUH observations, consistent with results over the tropical ocean (John *et al.* 2009). There is closer agreement in interannual coupling between CWV and T_s with strong, positive correlations in all datasets. The strongest response is evident in the observations (~ 5 – $6\% K^{-1}$), close to that expected from the Clausius–Clapeyron equation (Willett *et al.* 2008). Taking the ratio of CWV and T_s trends also results in a similar response ($\sim 7\% K^{-1}$) for SSM/I, HadCRUH and HadISST; the AMIP response is $5\% K^{-1}$ using the ratio method.

Moistening is also evident over the north Europe (Figure 5(e)) and Mediterranean (Figure 5(f)) regions (Tables I and II), despite declining relative humidity

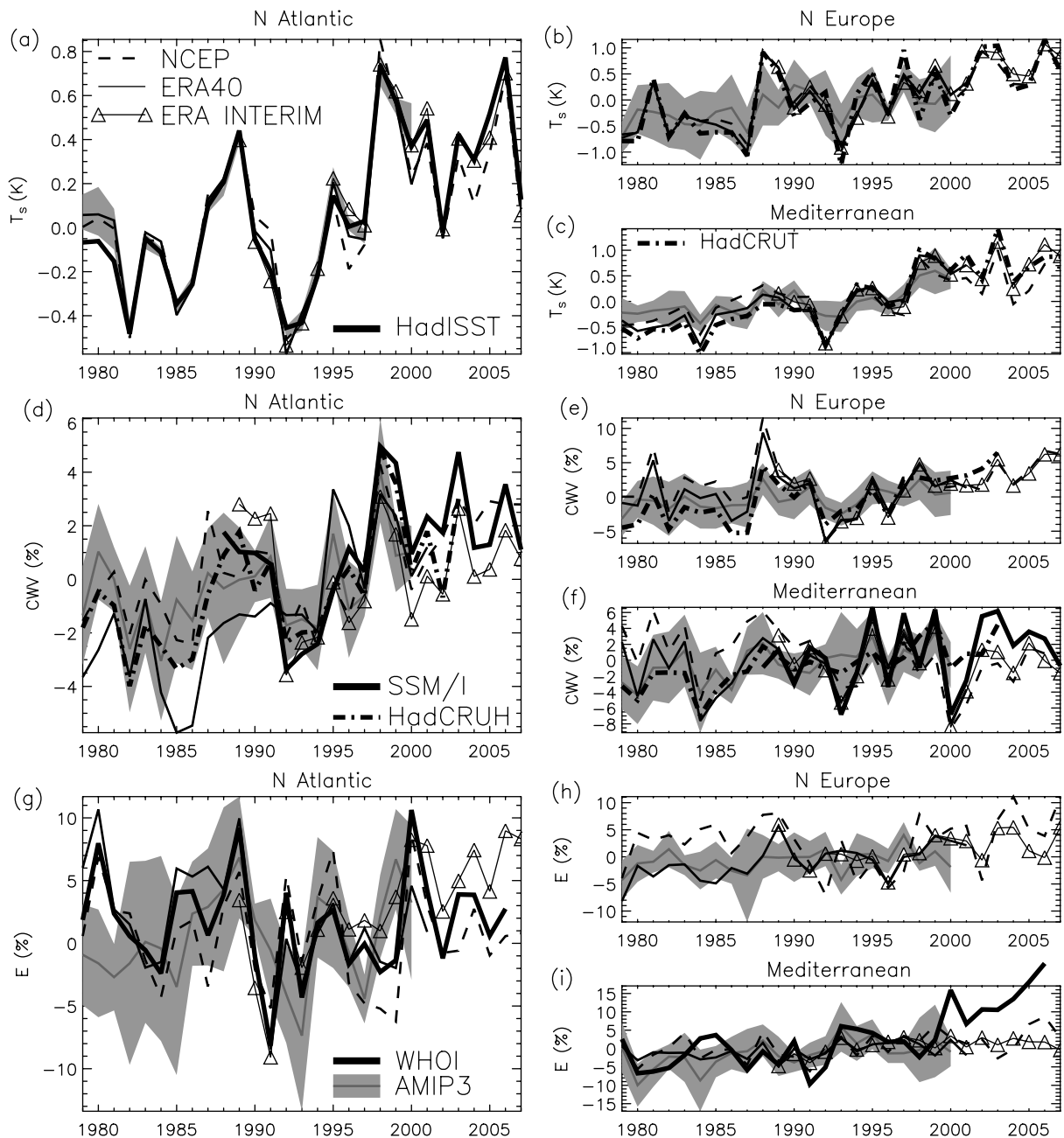


Figure 5. As Figure 2 but for anomalies of surface temperature (a)–(c), column integrated water vapour (d)–(f) and surface evaporation (g)–(i).

(Willett *et al.* 2008). The strongest trends in CWV are over northern Europe for the HadCRUH and ERA Interim datasets (3.2% per decade), larger than the AMIP models; NCEP and ERA40 did not reveal significant trends. However, all datasets considered showed a strong relationship with T_s , ranging from ~ 3 – $5\% K^{-1}$. Taking the ratio of water vapour and T_s trends, the HadCRU/HadISST data suggest a sensitivity $\sim 7\% K^{-1}$, close to Clausius–Clapeyron; smaller trends are evident for ERA Interim ($6\% K^{-1}$) and the AMIP models ($4\% K^{-1}$).

Over the Mediterranean region CWV trends and sensitivity to T_s are larger for AMIP3 but smaller for HadCRUT but with both datasets indicating pronounced moistening. Taking the ratio of trends, CWV increases at $6.2\% K^{-1}$ in the models, close to Clausius–Clapeyron,

but at a lower rate in the observations ($4\% K^{-1}$). The reanalysis datasets suggest only weak CWV trends and links to warming over the Mediterranean. The moistening trends in the HadCRUT and SSM/I datasets and AMIP models are also consistent with radiosonde data (Durre *et al.* 2009) which suggests a 0.45 mm/decade trend over northern hemisphere land since 1973 although the trend over Europe in summer is 0.18 mm/decade (around 1% per decade) and not statistically significant.

Substantial interannual variability in E is evident over the Atlantic region (Figure 5(g)) but trends are incoherent (Table II). The WHOI observations display only a weak dependence of E upon T_s while a stronger dependence, close to the Clausius–Clapeyron rate ($\sim 7\% K^{-1}$) is simulated by the AMIP model ensemble and ERA

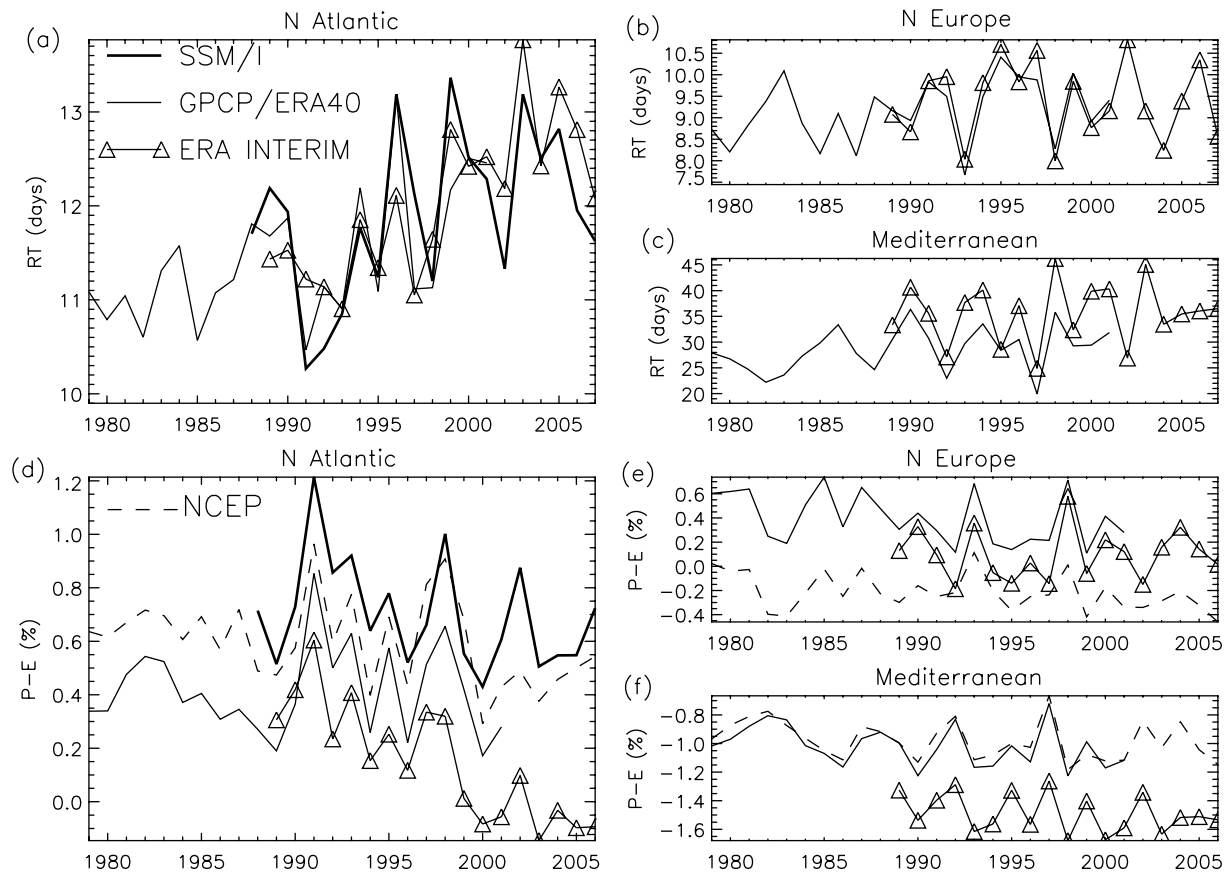


Figure 6. As Figure 2 but for residence time (days) and precipitation – evaporation (mm day^{-1}).

Interim data (Table II). Positive coupling between E and T_s is more robust across reanalyses and models for the north European region (Table II) but links with T_s are significant only for ERA40. Conversely, over the Mediterranean region, coupling between E and T_s is weak while trends are positive in all datasets. The AMIP3 models (Table I) simulate stronger trends and variability than the reanalyses. The WHOI ocean-only data also indicates substantial increases in E , especially after 1998.

The rising CWV, declining P and relatively stable E over the Atlantic ocean region result in a positive trend in water vapour residence time (CWV/P) and negative trends in $P - E$ in all datasets (Figure 6). It is misleading to interpret these changes in the water vapour residence time as an intrinsic property of the hydrologic cycle; rather it is an informative diagnostic of the regional water cycle, affected by moisture transport as well as local recycling of moisture (e.g. Schär *et al.* 1999). A peak in $P - E$ is evident in 1991 and declines thereafter. Longer term changes in these variables over north Europe and the Mediterranean regions are less coherent.

5. Spatial anomalies in 1991 and 2007

We now analyse in more detail the spatial structure of anomalies in aspects of the hydrological cycle for summer

1991 over the Atlantic (Figure 7) and 2007 over the whole region (Figure 8).

Summer 1991 over the north Atlantic was characterized by anomalously high $P - E$ (Figure 6(d)). The positive P (SSM/I) and negative E (WHOI) anomalies are associated with a negative surface pressure anomaly centred at 40°W , 55°N with anomalous ascent on the southern and eastern flanks of the anomaly and reduced wind speed to the south (Figure 7). The negative T_s anomaly off Newfoundland (Figure 7(b)), a region thought to be important in influencing multi-decadal variations in summer climate (Sutton and Hodson 2005), is associated with anomalous northerly wind flow. The positive $P - E$ is also consistent with negative salinity anomalies in the early 1990s (Belkin 2004). While the effect of the Pinatubo volcanic eruption in June 1991 was unlikely to have influenced the north-Atlantic climate during this immediate period, the anomalous conditions may have been linked to an emerging Atlantic El Niño-like event (Polonsky 1994).

During summer 2007, P anomalies of 10% over northern Europe (from GPCP) coincided with a negative phase of the NAO (Figure 2(b)), with a broadly similar pattern of precipitation differences to the positive minus negative NAO phase shown in Figure 1(b). Increased P mainly affected north-west Europe and northern European Russia, yet were not associated with stronger ascent (Figure 8(a)). This is possibly because the intense rainfall

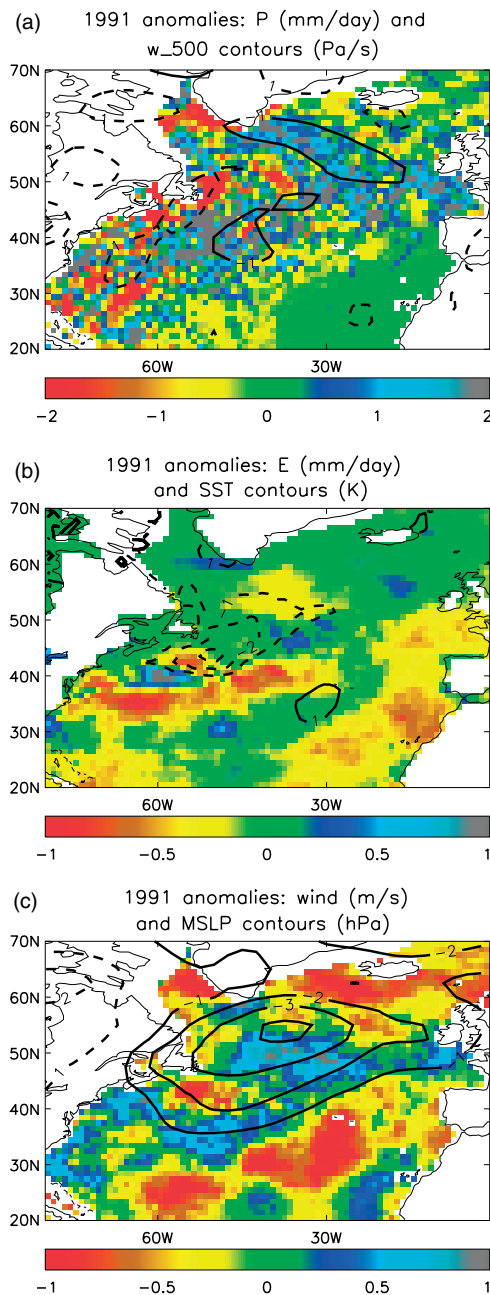


Figure 7. Observed anomalies of (a) SSM/I precipitation and NCEP vertical motion, (b) WHOI surface evaporation and HadISST temperature and (c) SSM/I wind speed and NCEP sea level pressure for summer 1991.

originated from a small number of intense precipitation events (Blackburn *et al.* 2008). Evaporation anomalies from NCEP coincide with P anomalies over land regions with around half of the additional P being lost through evapotranspiration. Evaporation anomalies were also positive over the Atlantic between 30 and 40°N, a source region for the air masses important in delivering intense rainfall to the UK during June–July 2007 (Blackburn *et al.* 2008). Negative E anomalies were present over the north-west Atlantic and eastern Mediterranean, coinciding with anomalous warmth (Figure 8(b)). Evaporation anomalies are also linked with wind anomalies (from

SSM/I), negative over the north Atlantic, positive over the south-east of the north Atlantic region, themselves associated with anomalously high surface pressure in the north and low pressure in the south-east of the region (Figure 8(c)).

Mean sea level pressure was anomalously low over northern Europe during summer 2007 (Figure 3(e)), in particular over north-west Europe (Figure 8). The persistence of an upper level trough over this region is thought to have been instrumental in determining the intense rainfall events over the UK during this period (Blackburn *et al.* 2008).

6. Conclusions

Variability in aspects of the hydrological cycle is analysed over the north Atlantic, north Europe and Mediterranean regions during the summer season for the period 1979–2007, using observational estimates, reanalyses and climate model simulations. Warming trends are present in all datasets for all regions although the model simulations underestimate trends over Europe, demonstrating that only some of the warming across Europe is explained by the sea surface temperature and sea ice forcing prescribed in these experiments. Reduced aerosol cooling over land (Wild *et al.* 2008) and over the subtropical north Atlantic (Evan *et al.* 2009), and direct forcing by greenhouse gases, not represented by the models, may contribute to this underestimate (Philipona *et al.* 2009). Further comparisons with atmosphere-only models and fully coupled models in which greenhouse gas and realistic aerosol forcings applied are required to clarify the magnitude of these effects further.

Moistening trends are also captured by the models and observations, with observed changes in water vapour rising at the rate expected from Clausius–Clapeyron ($7\% K^{-1}$) over the north Atlantic and north Europe region, consistent with Willett *et al.* (2008), and slightly below this rate in the models ($4\text{--}5\% K^{-1}$). Reanalysis products, including ERA Interim, struggle to represent decadal changes as discussed previously by Bengtsson *et al.* (2004).

Over Europe, warmer conditions favour higher moisture amounts, implying greater rainfall intensity (e.g. Trenberth *et al.* 2003), yet the warmer conditions in summer are a likely occurrence of drier cloud-free conditions (e.g. Trenberth and Shea 2005). On the basis of the present analysis, the latter effect appears to dominate, in particular over the Mediterranean, where P is negatively correlated with T_s . Declining summer rainfall over Europe has also been observed over recent decades from observations and is consistent with future climate projection (Pal *et al.* 2004).

Precipitation variability over Europe is dominated by the large-scale dynamics; positive phases of the summer NAO index are associated with reduced P over north Europe and wetter conditions across the Mediterranean region, in agreement with Folland *et al.*

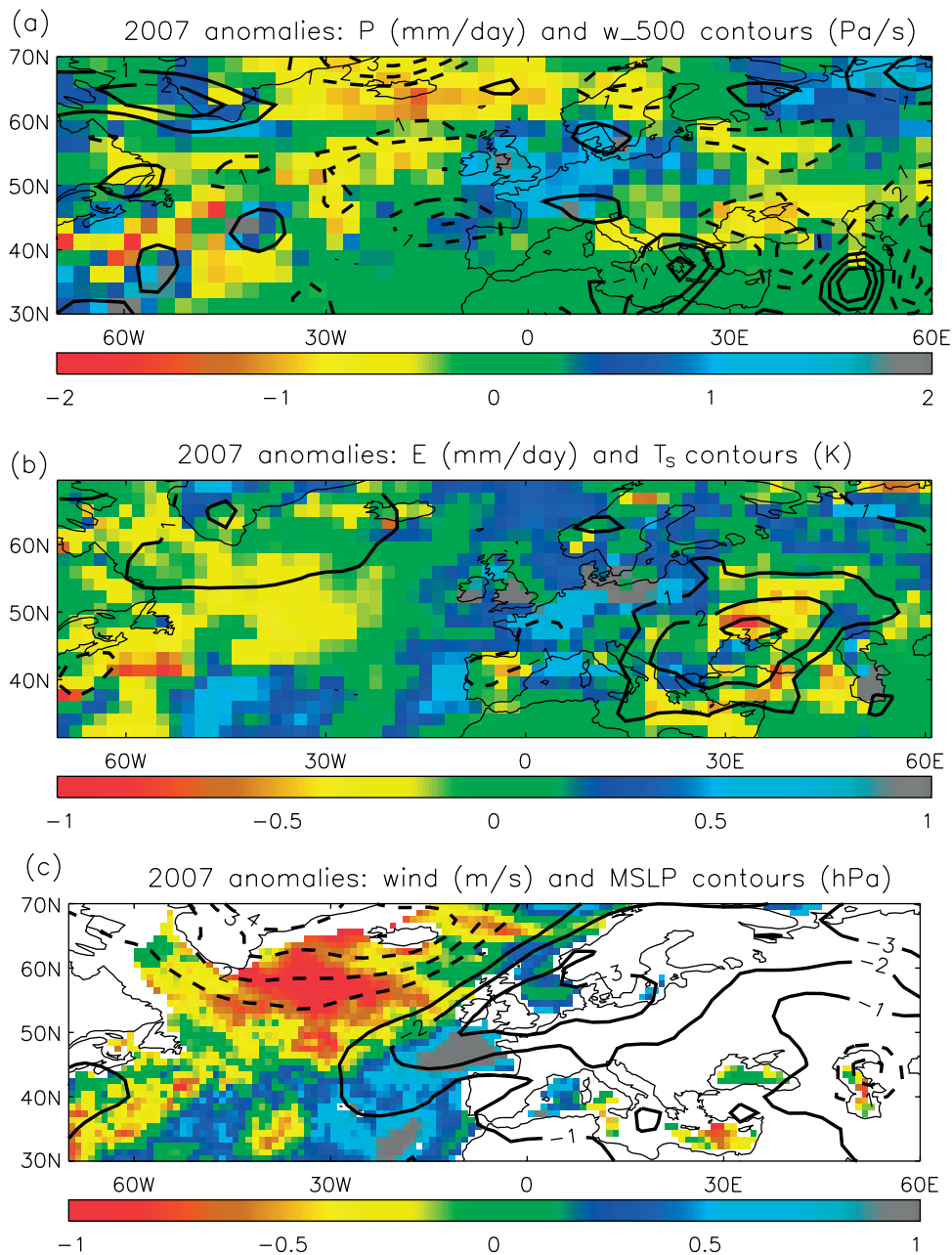


Figure 8. Anomalies of (a) GPCP precipitation and NCEP vertical motion, (b) NCEP surface evaporation and temperature and (c) SSM/I wind speed and NCEP sea level pressure for summer 2007.

(2009). Evaporation trends over Europe from models and reanalyses are positive (1–3% per decade), in particular for the Mediterranean region with the models displaying the largest variability and trends in this region.

There is evidence of declining P over the north Atlantic region in all datasets although with substantial variability ($\pm 10\%$). Rising moisture yet declining P explain substantial rises in water vapour residence time, of around 2 days, over the north Atlantic in all datasets considered. This is consistent with model projections over the 21st century which are influenced by a poleward expansion of the sub-tropical high pressure regimes (Christensen *et al.* 2007). Maximum $P - E$ over the north Atlantic occurred during summer 1991, associated with a negative pressure anomaly, but declined

thereafter. Changes in $P - E$ over the Atlantic may have contributed to ocean salinity anomalies during the 1990s (Belkin 2004) and it is crucial to understand the links between Atlantic Ocean temperature and salinity and decadal changes in summer climate over Europe associated with the Atlantic Multi-decadal Oscillation (Sutton and Hodson 2005), the signal of which is most pronounced in the summer season (Delworth and Mann 2000).

Finally, it is important to note the limitations of analysing changes in aspects of the water cycle over recent decades across the Atlantic-Europe sector. Homogenizing conventional and satellite datasets is problematic (e.g. Willett *et al.* 2008; Brohan *et al.* 2006; Yu and Weller 2007; Bengtsson *et al.* 2004) and the

combination of a variety of observations, reanalysis and model products is essential in monitoring climate regionally and globally. Also, determining the mechanism of regional change over a decadal time-scale is difficult as variability relates to a combination of circulation changes, climate forcings, such as greenhouse gases and aerosol, and feedbacks relating to water vapour, cloud and the land surface (e.g. Philipona *et al.* 2009). The application of regional models up to fully coupled global models is necessary to understand mechanisms influencing European summer climate (e.g. Schär *et al.* 1999; Koster *et al.* 2004; Sutton and Hodson 2005).

acknowledgements

This research was supported by the Royal Society grant H5046100 and the UK NERC grant NE/C51785X/1 and National Centre for Earth Observation. The input of two anonymous reviewers helped to improve the paper. GPCP data were extracted from www.ncdc.noaa.gov; SSM/I data were provided by Remote Sensing Systems; NCEP data from www.ncdc.noaa.gov; ECMWF data from www.ecmwf.int; WHOI data from the Woods Hole Oceanographic institute; HadCRUH and HadISST data was supplied by the Met Office. The AMIP3 model data was provided by the WCRP and PCMDI.

References

- Adler RF, Gu G, Wang J-J, Huffman GJ, Curtis S, Bolvin D. 2008. Relationships between global precipitation and surface temperature on interannual and longer timescales (1979–2006). *Journal of Geophysical Research* **113**: Art. no. D22104, DOI:10.1029/2008JD010536.
- Allan RP, Ringer MA, Pament JA, Slingo A. 2004. Simulation of the Earth's radiation budget by the European Centre for Medium Range Weather Forecasts 40-year reanalysis (ERA40). *Journal of Geophysical Research* **109**(D05105): 232, DOI:10.1029/2004JD005.
- Allan RP, Soden BJ. 2007. Large discrepancy between observed and simulated precipitation trends in the ascending and descending branches of the tropical circulation. *Geophysical Research Letters* **34**: Art. no. L18705, DOI:10.1029/2007GL031460.
- Belkin IM. 2004. Propagation of the Great Salinity Anomaly of the 1990s around the northern north atlantic. *Geophysical Research Letters* **31**(8): Art. no. L08306, DOI:10.1029/2003GL019334.
- Bengtsson L, Hagemann S, Hodges KI. 2004. Can climate trends be calculated from reanalysis data? *Journal of Geophysical Research-Atmospheres* **109**(D11): Art. no. D11111, DOI:10.1029/2004JD004536.
- Blackburn M, Methven J, Roberts N. 2008. Large-scale context for the UK floods in summer 2007. *Weather* **63**(9): 280–288.
- Brohan P, Kennedy JJ, Harris I, Tett SFB, Jones PD. 2006. Uncertainty estimates in regional and global observed temperature changes: a new data set from 1850. *Journal of Geophysical Research* **111**: Art. no. D12106, DOI: <http://dx.doi.org/10.1029/2005JD006548>.
- Christensen JH, Hewitson B, Busiuc A, Chen A, Gao X, Held I, Jones R, Kolli RK, Kwon W-T, Laprise R, Magaña Rueda V, Mearns L, Menéndez CG, Räisänen J, Rinke A, Sarr A, Whetton P. 2007. Regional climate projections. *Climate Change 2007: The Physical Science Basis*. Contribution of Working Group I to the Fourth Assessment Report of the Intergovernmental Panel on Climate Change. Cambridge University Press: Cambridge, UK, New York; 847–940.
- Collins WD, Bitz CM, Blackmon ML, Bonan GB, Bretherton CS, Carton JA, Chang P, Doney SC, Hack JJ, Henderson TB, Kiehl JT, Large WG, McKenna DS, Santer BD, Smith RD. 2006. The Community Climate System Model version 3 (CCSM3). *Journal of Climate* **19**: 2122–2143.
- Dai A. 2006. Recent climatology, variability, and trends in global surface humidity. *Journal of Climate* **19**: 3589–3606.
- Delworth TL, Mann ME. 2000. Observed and simulated multidecadal variability in the northern hemisphere. *Climate Dynamics* **16**: 661–676.
- Durre I, Williams CN, Yin X, Vose RS. 2009. Radiosonde-based trends in precipitable water over the northern hemisphere: an update. *Journal of Geophysical Research-Atmospheres* **114**(D5): Art. no. D05112, DOI:10.1029/2008JD010989.
- Evan AT, Vimont DJ, Heidinger AK, Kossin JP, Bennartz R. 2009. The role of aerosols in the evolution of tropical north Atlantic ocean temperature anomalies. *Science*: Art. no. 1167404. **324**(5928): 778–781, DOI:10.1126/science.1167404.
- Folland CK, Knight J, Linderholm HW, Fereday D, Ineson S, Hurrell JW. 2009. The summer north atlantic oscillation: past, present, and future. *Journal of Climate* **22**(5): 1082–1103.
- Hasumi H, Emori S. 2004. K-1 coupled model (MIROC) description. Technical Report no. K-1, Tech. Report no 1. Center for Climate System Research, University of Tokyo: 34 pp.
- John VO, Allan RP, Soden BJ. 2009. How robust are observed and simulated precipitation responses to tropical warming. *Geophysical Research Letters* **36**: Art. no. L14702, DOI:10.1029/2009GL038276.
- Kalnay E, Kanamitsu M, Kistler R, Collins W, Deaven D, Gandin L, Iredell M, Saha S, White G, Woollen J, Zhu Y, Chelliah M, Ebisuzaki W, Higgins W, Janowiak J, Mo KC, Ropelewski C, Wang J, Leetmaa A, Reynolds R, Jenne R, Joseph D. 1996. The NCEP/NCAR 40-year reanalysis project. *Bulletin of the American Meteorological Society* **77**: 437–471.
- Koster RD, Dirmeyer PA, Guo ZC, Bonan G, Chan E, Cox P, Gordon CT, Kanae S, Kowalczyk E, Lawrence D, Liu P, Lu CH, Malyshev S, McAvaney B, Mitchell K, Mocko D, Oki T, Oleson K, Pitman A, Sud YC, Taylor CM, Verseghy D, Vasic R, Xue YK, Yamada T. 2004. Regions of strong coupling between soil moisture and precipitation. *Science* **305**(5687): 1138–1140.
- Lenderink G, Van Meijgaard E. 2008. Increase in hourly precipitation extremes beyond expectations from temperature changes. *Nature Geoscience* **1**: 511–514, DOI:10.1038/ngeo262.
- Marti O, Braconnot P, Bellier J, Benschila R, Bony S, Brockmann P, Cadule P, Caubel A, Denvil S, Dufresne J-L, Fairhead L, Filiberti M-A, Foujols M-A, Fichet F, Friedlingstein P, Goosse H, Grandpeix J-Y, Hourdin F, Krinner G, Lévy C, Madec G, Musat I, de Noblet N, Polcher J, Talandier C. 2005. The new IPSL climate system model: IPSL-CM4. Technical Report No 26. Institut Pierre Simon Laplace des Sciences de l'Environnement Global: IPSL, Case 101, Paris, France. .
- Pal JS, Giorgi F, Bi X. 2004. Consistency of recent european summer precipitation trends and extremes with future regional climate projections. *Geophysical Research Letters* **31**(13): Art. no. L13202, DOI:10.1029/2004GL019836.
- Philipona R, Behrens K, Ruckstuhl C. 2009. How declining aerosols and rising greenhouse gases forced rapid warming in Europe since the 1980s. *Geophysical Research Letters* **36**: Art. no. L02806, DOI:10.1029/2008GL036.
- Polonsky AB. 1994. Comparative study of the Pacific ENSO event of 1991–92 and the Atlantic ENSO-like event of 1991. *Australian Journal of Marine and Freshwater Research* **45**: 705–725.
- Rayner NA, Parker D, Horton E, Folland C, Alexander L, Rowell D, Kent E, Kaplan A. 2003. Global analysis of sst, sea ice and night marine air temperature since the late nineteenth century. *Journal of Geophysical Research* **108**: 4407, DOI:10.1029/2002JD002670.
- Salas-Méllia D, Chauvin F, Déqué M, Douville H, Guérémy JF, Marquet P, Planton S, Royer JF, Tyteca S. 2005. Description and validation of the CNRM-CM3 global coupled model. Technical Report CNRM working note 103. Météo-France: 42 Avenue Gaspard Coriolis, 31057 Toulouse Cedex, France, 36 pp.
- Schär C, Lüthi D, Beyerle U. 1999. The soil-precipitation feedback: a process study with a regional climate model. *Journal of Climate* **12**: 722–741.
- Schar C, Vidale PL, Luthi D, Frei C, Haberli C, Liniger MA, Appenzeller C. 2004. The role of increasing temperature variability in european summer heatwaves. *Nature* **427**(6972): 332–336.
- Sutton RT, Hodson DL. 2005. Atlantic Ocean forcing of North American and European summer climate. *Science* **309**(5731): 115–118.
- Trenberth KE, Dai A, Rasmussen RM, Parsons DB. 2003. The changing character of precipitation. *Bulletin of the American Meteorological Society* **84**: 1205–1217.

- Trenberth KE, Fasullo J, Smith L. 2005. Trends and variability in column-integrated atmospheric water vapor. *Climate Dynamics* **24**: 741–758.
- Trenberth KE, Shea DJ. 2005. Relationships between precipitation and surface temperature. *Geophysical Research Letters* **32**(14): L14 703+, DOI:10.1029/2005GL022760.
- Trenberth KE, Jones PD, Ambenje P, Bojariu R, Easterling D, Klein Tank A, Parker D, Rahimzadeh F, Renwick JA, Rusticucci M, Soden B, Zhai P. 2007. *Observations: Surface and Atmospheric Climate Change*. Climate Change 2007: The Physical Science Basis. Contribution of Working Group I to the Fourth Assessment Report of the Intergovernmental Panel on Climate Change. Cambridge University Press: Cambridge, United Kingdom and New York; 235–336.
- Uppala SM, Kallberg PW, Simmons AJ, Andrae U, Bechtold VD, Fiorino M, Gibson JK, Haseler J, Hernandez A, Kelly GA, Li X, Onogi K, Saarinen S, Sokka N, Allan RP, Andersson E, Arpe K, Balmaseda MA, Beljaars ACM, Van De Berg L, Bidlot J, Bormann N, Caires S, Chevallier F, Dethof A, Dragosavac M, Fisher M, Fuentes M, Hagemann S, Holm E, Hoskins BJ, Isaksen I, Janssen PAEM, Jenne R, McNally AP, Mahfouf JF, Morcrette JJ, Rayner NA, Saunders RW, Simon P, Sterl A, Trenberth KE, Untch A, Vasiljevic D, Viterbo P, Woollen J. 2005. The ERA-40 re-analysis. *Quarterly Journal of the Royal Meteorological Society* **131**: 2961–3012.
- Wentz FJ, Ricciardulli L, Hilburn K, Mears C. 2007. How much more rain will global warming bring? *Science* **317**: 233–235.
- Wild M, Grieser J, Schär C. 2008. Combined surface solar brightening and increasing greenhouse effect favour recent intensification of the hydrological cycle. *Geophysical Research Letters* **35**: Art. no. L17706, DOI:10.1029/2008GL034842.
- Willett KM, Jones PD, Gillett NP, Thorne PW. 2008. Recent changes in surface humidity: development of the HadCRUH dataset. *Journal of Climate* **21**(20): 5364–5383.
- Yu L, Weller RA. 2007. Objectively analyzed air-sea heat fluxes for the global ice-free oceans (1981–2005). *Bulletin of the American Meteorological Society* **88**: 527–539.
- Yukimoto S, Noda A. 2002. Improvements in the Meteorological Research Institute Global Ocean-Atmosphere Coupled GCM (MRI-CGCM2) and its climate sensitivity. Technical Report no. 10. NIES, Japan: 8 pp.
- Zveryaev II. 2006. Seasonally varying modes in long-term variability of European precipitation during the 20th century. *Journal of Geophysical Research-Atmospheres* **111**(D21): Art. no. D21116, DOI:10.1029/2005JD006821.
- Zveryaev II, Allan RP. 2009. Summertime precipitation variability over Europe and its links to atmospheric dynamics and evaporation. *Journal of Geophysical Research* (in press), DOI:10.1029/2008JD011213.
- Zveryaev II, Wibig J, Allan RP. 2008. Contrasting interannual variability of atmospheric moisture over Europe during cold and warm seasons. *Tellus A* **60**(1): 32–41, DOI:10.1111/j.1600-0870.2007.00283.x.